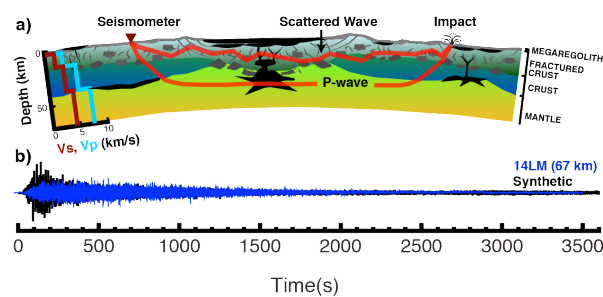


**SEISMIC PROPERTIES OF THE LUNAR MEGAREGOLITH.** N. C. Schmerr<sup>1</sup>, M. S. Thorne<sup>2</sup>, and Y. Yao<sup>2</sup>, <sup>1</sup>NASA-GSFC Greenbelt, MD 20771 USA [nicholas.c.schmerr@nasa.gov](mailto:nicholas.c.schmerr@nasa.gov), <sup>2</sup>Dept. of Geology & Geophysics, University of Utah, Salt Lake City, Utah, U.S.A [michael.thorne@utah.edu](mailto:michael.thorne@utah.edu), [yao.yao@utah.edu](mailto:yao.yao@utah.edu).

**Introduction:** The thickness and structure of the lunar crust are key constraints on the bulk composition, evolution, and formation of the Moon [1]. Over the past 4.5 billion years, the primarily anorthositic lunar crust has been modified by mare volcanism and extensive impact cratering, creating a non-uniform layer of megaregolithic materials overlying fractured and faulted crustal rock [2]. Past constraints on the thickness of the megaregolith layer are provided by seismic and gravity measurements; these indicate the layer is between 1-3 km thick [3], with impact fracturing and related faults possibly extending into the lunar mantle [Fig. 1]. Here we combine measurements of lunar seismic codas produced by scattering of elastic waves within the porous and unconsolidated materials of the megaregolith to study the thickness and elastic properties of this layer.



**Figure 1.** Seismic waves in schematic of lunar crustal structure. a) Seismic velocity model of the lunar crust from [4] and raypaths of direct and scattered waves. b) Seismogram recorded at the Apollo 14 PSE station, showing the waveform of the impact of the Apollo 14 lunar module (blue) and a 1-D synthetic seismogram (black) [5].

*Background.* Recently, NASA's Gravity Recovery and Interior Laboratory (GRAIL) has provided new high-resolution maps of variations in lunar gravity, including constraints on crustal density, porosity, and thickness of the crust [6, 7]. The bulk crustal densities and lateral variations retrieved by GRAIL are on the order of  $2550 \pm 250 \text{ kg m}^{-3}$ , considerably less than the  $2800\text{-}2900 \text{ kg m}^{-3}$  that are typical for anorthositic crustal materials [6]. This low density requires a considerable amount of porosity (4-21%) in the lunar crust, likely resulting from the extensive impact gardening of lunar crustal materials. Porosity arises from fracturing of crustal rocks (i.e., cracks, joints, and faults), as well as intragranular pore space in poorly consolidated ejecta fragments and brecciated sedimen-

tary materials; the gravity constraints do not uniquely constrain the distribution in depth of porosity [8].

Seismic observations of megaregolith structure are provided by the Apollo Passive Seismic Experiment (APSE), a four station seismic network deployed on the nearside of the Moon by the Apollo 12, 14, 15, and 16 astronauts, the Active Seismic Experiment (ASE) from Apollo 14 and 16, and Lunar Seismic Profiling Experiment (LPSE) from Apollo 17. The APSE consisted of four stations, in operation from 1969 until 1977, arranged in the form of a 1200 km equilateral triangle, with Apollo 12 and 14 sites located at one vertex of the triangular array [9]. The two ASE deployments consisted of 3 geophones spaced  $\sim 46 \text{ m}$  apart, with sources including an explosive charge powered thumper, and four sequential mortar shots out to 900 m away from the experiment [10]. The LPSE was similar to the ASE with the exception that the geophone array had a much larger aperture of 3.5 km [11].

The PSE, ASE, and LPSE provided seismic measurements of the thickness and elastic properties of the lunar megaregolith, indicating the layer is  $\sim 3 \text{ km}$  thick beneath the Apollo stations, with seismic wave velocities on the order of  $300 \text{ m s}^{-1}$  [12]. The lowered seismic velocities of the megaregolith are similar to those observed near impact craters on Earth, and are related to the high amount of pore space lowering the rigidity and compressibility of fractured and brecciated rock. However, it is uncertain how deeply this fracturing extends into the lunar crust. In addition, seismic waves passing through fractured materials will be highly scattered, producing long duration codas of energy that typically decay with travel time [13]. This is characteristic of lunar seismograms; the relatively low attenuation of seismic waves in the lunar interior produces codas that extend over 1-hour or longer [14] [Fig. 1]. Here we use a 3-D wave propagation method to investigate the depth extent of scattering and compare the modeling results to Apollo seismic data and GRAIL gravity constraints of megaregolith and crust.

**Approach:** Forward modeling of scattering effects requires the consideration of 3-D wave propagation, an approach that has become routinely accessible with large-scale parallel processing and increased processor speeds. To model the effects of megaregolith heterogeneity on wave propagation in the moon, we have adapted the 3-D Cartesian finite difference code Serpentine Wave Propagation Program (WPP) for lunar elastic parameters and radius [15]. WPP allows us to

investigate the effects of scattering at frequencies  $\leq 2$  Hz for 3-D lateral and vertical heterogeneities in the lunar crust. We run WPP to obtain lunar scatterograms. This approach is benchmarked against synthetic seismograms from a lunar adapted reflectivity code [5] using a background reference structure constructed from a weighted average travel time fit of 1-D lunar velocity models [16].

With WPP, we explore a model space where the depth extent and strength of crustal porosity is varied in a Cartesian box. Porosity translates to lateral variations in seismic wave speeds and scattering effects; we introduce up to 25% heterogeneity in seismic wavespeeds to simulate increasing porosity level in the model [14]. Stations are spaced every 50 m at the surface of the model to facilitate comparison of the resulting seismograms with data from both the PSE and ASE experiments [Fig. 2].

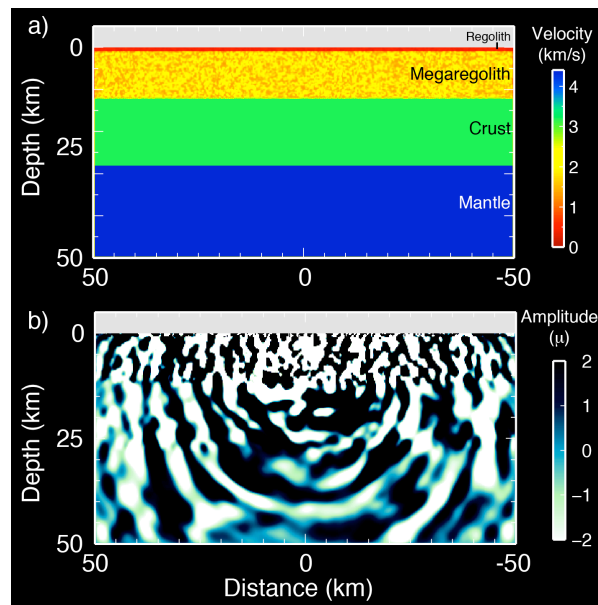


**Fig. 2:** Vertical cross section through a 2 Hz WPP simulation. a) Velocity model of Garcia et al., [4] with  $\pm 25\%$  heterogeneity in a von Karman type media [17] in the upper 12.5 km of the model. b) Displacement snapshot at 30 seconds into the simulation. The 4.0  $M_w$  source implemented at 0 km depth with an explosion type radiation pattern. Grid spacing is 200 m with refinements at 10 and 3 km depth.

**Comparison to Data:** Forward modeled seismograms are compared to the artificial impact data recorded at the Apollo stations [Fig. 1]. The origin times and epicenters of the artificial impacts are precisely known from telemetry and direct detection of the impact craters [18], allowing us to control for source effects in our measurements. Seismogram processing

includes despiking, band-pass filtering, enveloping of amplitudes, and calculating a moving time window average of the enveloped amplitudes. Synthetic seismograms are processed using the same approach as the data. We estimate coda rise times by picking the first arrival and subsequent peak time. The coda decay is quantified by fitting a 2<sup>nd</sup> order polynomial fit to the enveloped seismic trace. These observational values will be used to constrain the depth and extent of porosity in the megaregolith through comparison with the synthetic coda rise times and decay slopes.

**Further Implications:** Our study will constrain the depth extent of the fracturing and bedrock disruption in the Moon and the associated crustal porosities, significantly reducing the uncertainties in models of density distribution in the lunar crust. Density distribution is an important constraint for studying global gravity models of crustal thickness and our seismic observations will serve to provide a baseline for future gravity models [6]. In addition, seismic scattering is a major process present in the megaregolith of other planetary objects. This approach can be used to establish the detailed character of the seismic wavefield at the proposed locations of potential landing sites of future seismometer deployments.

**References:** [1] Wieczorek, M. A. (2009) *Elements* 5, 35 10.2113/gselements.5.1.35. [2] Toksoz, M. N. et al. (1972) *Science* 176, 1012. [3] Nakamura, Y. (2011) *Journal of Geophysical Research-Planets* 116, E12005 10.1029/2011je003972. [4] Garcia, R. F. et al. (2011) *Phys Earth Planet Inter* 188, 96 10.1016/j.pepi.2011.06.015. [5] Fuchs, K. et al. (1971) *Geophys J Roy Astron Soc* 23, 417. [6] Wieczorek, M. A. et al. (2012) *Science*, 10.1126/science.1231530. [7] Zuber, M. T. et al. (2012) *Science*, 10.1126/science.1231507. [8] Huang, Q. et al. (2012) *Journal of Geophysical Research-Planets* 117, E05003 10.1029/2012je004062. [9] Latham, G. V. et al. (1969) *Transactions-American Geophysical Union* 50, 679. [10] Watkins, J. S. et al. (1972) *Science* 175, 1244 10.1126/science.175.4027.1244. [11] Kovach, R. L. et al. (1973) *Science* 180, 1063 10.1126/science.180.4090.1063. [12] Toksoz, M. N. et al. (1974) *Rev Geophys* 12, 539. [13] Rodriguez-Castellanos, A. et al. (2006) *Bull Seismol Soc Am* 96, 1359 10.1785/0120040138. [14] Dainty, A. M. et al. (1974) *Transactions-American Geophysical Union* 55, 362. [15] Petersson, N. A. et al. (2010) *Lawrence Livermore National Laboratory Technical Report LLNL-TR-422928*. [16] Yao, Y. et al. (2012) paper presented at the AGU Fall Meeting, San Francisco. [17] Frankel, A. et al. (1986) *Journal of Geophysical Research-Solid Earth and Planets* 91, 6465 10.1029/JB091iB06p06465. [18] Daubar, I. J. et al. (2011) *LPS XLII*, Abstract #2232.